



Milan, David J. and Schwendel, Arved C. ORCID logoORCID:
<https://orcid.org/0000-0003-2937-1748> (2021) Climate-change driven increased flood magnitudes and frequency in the British uplands: geomorphologically informed scientific underpinning for upland flood-risk management. *Earth Surface Processes and Landforms*, 46 (15). pp. 3026-3044.

Downloaded from: <https://ray.yorks.ac.uk/id/eprint/5455/>

The version presented here may differ from the published version or version of record. If you intend to cite from the work you are advised to consult the publisher's version:
<https://onlinelibrary.wiley.com/doi/10.1002/esp.5206>

Research at York St John (RaY) is an institutional repository. It supports the principles of open access by making the research outputs of the University available in digital form. Copyright of the items stored in RaY reside with the authors and/or other copyright owners. Users may access full text items free of charge, and may download a copy for private study or non-commercial research. For further reuse terms, see licence terms governing individual outputs. [Institutional Repositories Policy Statement](#)

RaY

Research at the University of York St John

For more information please contact RaY at
ray@yorks.ac.uk

Milan David (Orcid ID: 0000-0002-9914-2134)

Schwendel Arved (Orcid ID: 0000-0003-2937-1748)

Climate-change driven increased flood magnitudes and frequency in the British uplands: geomorphologically informed scientific underpinning for upland flood-risk management

David J. Milan¹ & Arved C. Schwendel²

⁽¹⁾Department of Geography, Geology and Environment, University of Hull, UK

(Corresponding Author)

d.milan@hull.ac.uk

⁽²⁾School of Humanities, York St John University, UK

a.schwendel@yorks.ac.uk

Keywords: Terrestrial LiDAR, DEM differencing, flood-risk management, geomorphic work, sensitivity, thresholds, gravel-bed river, sediment management, hydrodynamic modelling, climate change

This article has been accepted for publication and undergone full peer review but has not been through the copyediting, typesetting, pagination and proofreading process which may lead to differences between this version and the Version of Record. Please cite this article as doi: 10.1002/esp.5206

Abstract

Upland river systems in the UK are predicted to be prone to the effects of increased flood magnitudes and frequency, driven by climate change. It is clear from recent events that some headwater catchments can be very sensitive to large floods, activating the full sediment system, with implications for flood risk management further down the catchment. We provide a 15-year record of detailed morphological change on a 500-m reach of upland gravel-bed river, focusing upon the geomorphic response to an extreme event in 2007, and the recovery in the decade following. Through novel application of 2D hydrodynamic modelling we evaluate the different energy states of pre- and post-flood morphologies of the river reach, exploring how energy state adjusts with recovery following the event. Following the 2007 flood, morphological adjustments resulted in changes to the shear stress population over the reach, most likely as a direct result of morphological changes, and resulting in higher shear stresses. Although the proportion of shear stresses in excess of those experienced using the pre-flood DEM varied over the recovery period, they remained substantially in excess of those experienced pre-2007, suggesting that there is still potential for enhanced bedload transport and morphological adjustment within the reach. Although volumetric change calculated from DEM differencing does indicate a reduction in erosion and deposition volumes in the decade following the flood, we argue that the system still has not recovered to the pre-flood situation. We further argue that Thinhope Burn, and other similarly impacted catchments in upland environments, may not recover under the wet climatic phase currently being experienced. Hence systems like Thinhope Burn will continue to deliver large volumes of sediment further down

river catchments, providing new challenges for flood risk management into the future.

Introduction

Flash flooding, in upland and mountainous areas is one of the top-ranked causes of fatalities among natural disasters globally (Borga *et al.*, 2011).

Between 1980-2017, 6963 hydrological events occurred Worldwide resulting in almost 250 000 casualties, and resulting in close to USD 1020 billion in damage (Munich, 2018). Increased heavy precipitation at regional (Groisman *et al.*, 2004) and global scales (Groisman *et al.*, 2005; Beniston, 2009) is thought to be linked to global warming (Huntington, 2006; Allamano *et al.*, 2009; Wilby *et al.*, 2008), and coupled with land-use change (Barrera-Escoda and Llasat, 2015), the hazard imposed by flash flooding is expected to increase in frequency and severity (Kleinen and Petschel-Held, 2007; Beniston *et al.*, 2011). Flash floods in upland areas are often highly energetic, and able to transport large quantities of sediment, inducing significant morphological changes including significant channel widening (Lucia *et al.*, 2015; Surian *et al.* 2016; Ruiz-Villanueva *et al.*, 2018; Scorpio *et al.*, 2018), and increasing flood hazards downstream (Radice *et al.*, 2013; Marchi *et al.*, 2010).

In the UK, there has been renewed interest in the management of upland rivers, particularly with respect to the implementation of Natural Flood Management approaches, to address potential increases in flood magnitudes as a result of global climate change (Lane, 2017; Dadson *et al.*, 2017). Over the last decade, there have been unprecedented hydrological events, with associated geomorphic response, including the highest ever rainfall totals recorded in Honister Pass,

Cumbria following the Storm 'Desmond' floods in December 2015 (Heritage *et al.*, 2019). In February 2020 Storms 'Ciara', 'Denis' and 'Jorge' resulted in a new February monthly record for the UK, and record discharges being recorded on the River Cynon and Wye catchments in south Wales (Parry *et al.*, 2021). In addition, second or third highest flows were widespread across northern and western UK. Since the mid 1990s the UK has been experiencing a wet climatic phase, resulting in a flood-rich period. Although there are regional variations, climate change projections from the latest global and regional climate models predict greater rainfall maxima, and more frequent storms, particularly in the summer, and with greater winter rainfall totals in the upland areas of the UK (Murphy *et al.*, 2009; 2020).

Little is known about the geomorphic implications of the UK's current wet climatic phase and the potential implications of future climate change. As the most severe meteorological effects appear to be predicted for upland Britain (Murphy *et al.*, 2020), it would appear prudent to examine the effects of increased flood magnitudes upon sediment transfer and fluvial response, as this has implications for flood risk management further down river catchments in lowland areas. River channel flood-related maintenance associated with bedload transport deposition is estimated to cost the UK £1.1 billion annually, and can have a severe impact on infrastructure and local flood risk following extreme events (Lane *et al.*, 2017; Slater, 2016); and these costs are expected to increase further under future climate change scenarios (Dadson *et al.*, 2017)

There are a number of studies that have documented extreme geomorphic responses to storm events in upland Britain (e.g. Newson, 1980; Carling, 1986;

Harvey, 1986; Warburton, 2010; Milan, 2012; Warburton *et al.*, 2016; Joyce *et al.*, 2017; Heritage *et al.*, 2019). These studies demonstrate how formerly dormant upland systems can potentially become activated by intense storms, resulting in mobilisation of the full sediment system, inducing slope failures and activating stored floodplain alluvium, often reconnecting typically disconnected sediment systems (Fryirs, 2013), and enhancing sediment supply. Extreme floods drive high bed shear stresses that can mobilise significant quantities of sediment, including very coarse material, and transfer these considerable distances downstream, impacting infrastructure, and with implications for management of flood risk and contaminants (Foulds *et al.*, 2014). However, there are few if any long-term monitoring studies available to help elucidate longer-term response and 'recovery' of upland catchments. Recovery describes the trajectory of change toward an improved geomorphic condition (Brierly and Fryirs, 2009), and in upland landscapes the role of connectivity has been identified as being a key control (Harvey, 2007). Although understanding recovery is likely to be key to successful river management in the future, Lisenby *et al.* (2018) has highlighted that the concept has been under-researched. Hence the geomorphologically-driven scientific underpinning, needed for sustainable flood risk management in upland areas, is currently non-existent. Understanding sediment delivery in catchments that have experienced state-change events (*sensu* Phillips, 2014) will aid calibration of the next generation of flood risk management models allowing for sediment transport and morphological changes, not just in the short-term but also allowing for future flood risk scenarios to be predicted, as decadal scale data inform on likely sediment transport volumes. In addition, hydrodynamic modelling using high

resolution field-work-derived base models, may be used to increase public awareness of the dangers of flash floods (e.g. Skinner and Milan, 2018).

This paper focuses upon the geomorphic response and recovery of a 500 m reach of the Thinhope Burn, a third-order tributary to the South Tyne catchment in northern England, impacted by a large summer flood in 2007 (Milan, 2012). Regular topographic monitoring of the site since the flood is used to provide a geomorphic insight into geomorphic response and recovery during the UK's current wet climatic phase. The study continues one of the few investigations to attempt to quantify geomorphic recovery a decade on since an extreme event occurred in an upland gravel-bed river, that was capable of exceeding thresholds for sediment store activation and triggering channel change. The paper extends the analysis of the 2003-2011 data presented in Milan (2012); providing new data between 2011-2018, and hydraulic interpretations.

Specifically, this paper aims to:

- 1) Quantify geomorphic response and recovery to an extreme flood in an upland stream through an examination of volumetric changes (erosion and deposition) changes;
- 2) Examine how morphological changes both in response to the 2007 event and over the recovery phase, influence the population distribution of bed shear stress;
- 3) Explore conceptual geomorphic frameworks to explain geomorphic response of upland river systems to extreme events under changing climatic conditions.

Study site

This investigation focused on a 500 m reach of the Thinhope Burn, a small 12 km² tributary to the River South Tyne situated in the north Pennines in Cumbria, UK (Ordnance Survey National grid reference NY680550, latitude 54° 52' 48.31" N, longitude 2° 31' 09.57" W, 180-595 m above Ordnance Datum, Figure 1). The catchment is underlain by Carboniferous sandstones, limestones, and shales, overlain by till and peat. The river channel displays pool-riffle and rapid morphology (see Heritage *et al.*, in press), with a mean bed slope of 0.031 m/m. In July 2007 an extreme rainfall event triggered a flood an estimated peak of 60 m³s⁻¹ (Milan, 2012), that equated to approximately a 1 in 80 year event, based upon the grain size of dated historic flood deposits (berms, lobes and splays) (Macklin *et al.*, 1992). The flood mobilised the full third-order valley floor and initiated a peat slide in the headwaters. Immediately following the event the channel changed from a narrow 6 m wide single-thread sinuous channel into a multi-thread channel with a width in the region of ~25 m (Figure 2), and new boulder berms, lobes and splays were deposited (Milan, 2012). Monitoring the coarse sediment budget over time using a spatially distributed ground-survey approach (e.g. Fuller *et al.*, 2002; 2003a,b; 2005) permits geomorphic assessment of response, recovery, and return to steady-state conditions. Using this approach at Thinhope Burn, Milan (2012) showed an order of magnitude change in erosion and deposition volumes in response to the 2007 event, compared with baseline sediment budgets whilst the channel was at steady state prior to the flood.

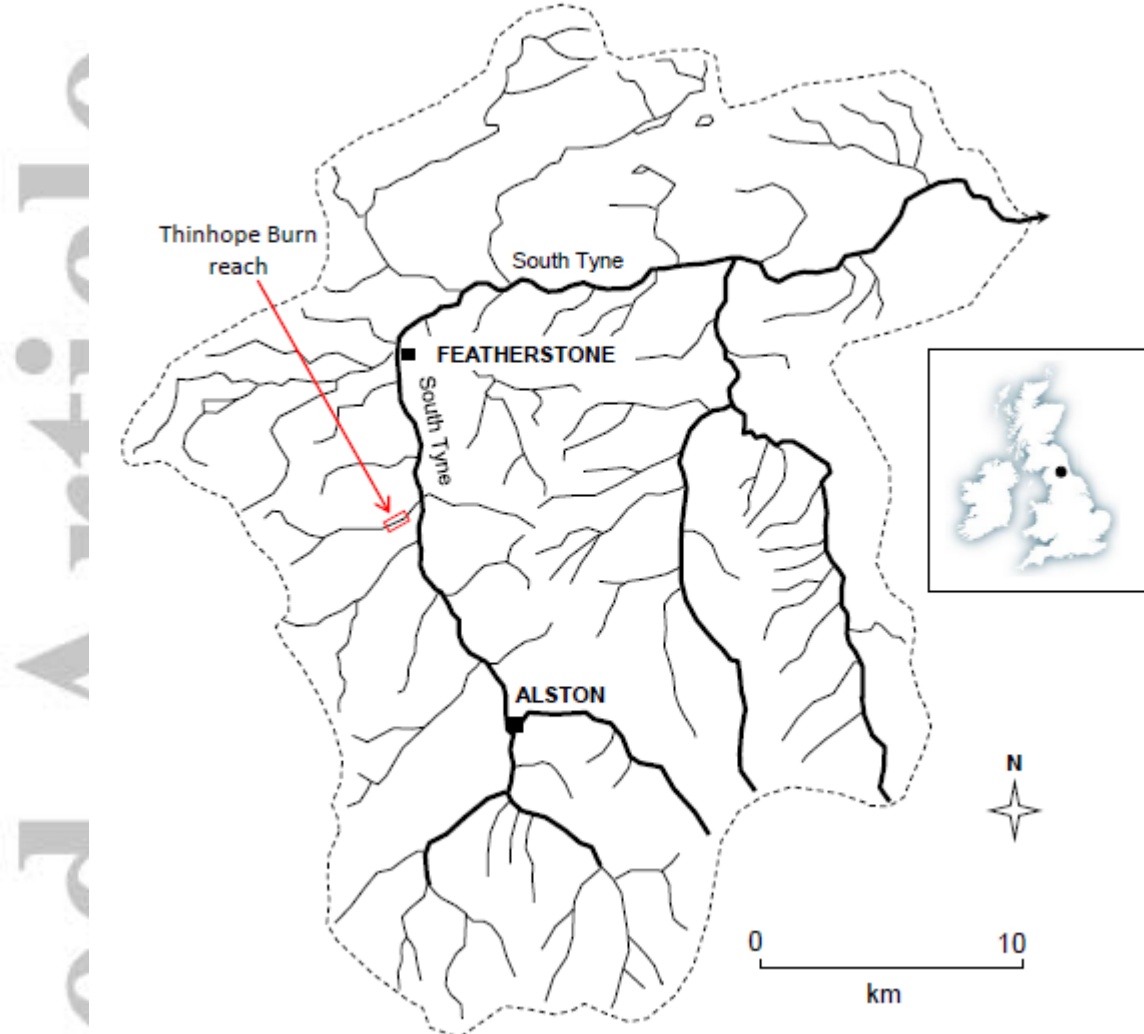


Figure 1 Study site location. Reach location on Thinhope Burn is indicated as the red box. The location of the gauging station used to generate data at Featherstone in Figure 3 is indicated.



Figure 2 Aerial photographs of study reach showing condition before the 2007 flood, immediately after and recovery a decade after the event. The cross-sections x and y on the 2006 image demonstrate the valley constriction from approximately 30 m to 15 m towards the tail-end 80 m of the reach. Source: Google Earth.

Although Thinhope Burn is not gauged, flow data exists for the South Tyne itself at Featherston approximately 4.7 km downstream of the confluence with the South Tyne (Figure 1). Peak flow data are of key interest in this study, and annual peak flows since 1966 are plotted in Figure 3. Between 1966 and 1993 the maximum flow was $310 \text{ m}^3\text{s}^{-1}$. Since 1993 there have been seven years where peak flows have exceeded this figure. Notably the peak flows in 2004, 2011, 2012 and 2015 all exceeded $400 \text{ m}^3\text{s}^{-1}$, with the 2012 peak flow exceeding $500 \text{ m}^3\text{s}^{-1}$. There is a strong suggestion that the change in hydrology is linked to the current wet phase in UK climate, that is predicted to be most pronounced in upland areas in the winter months (Dadson *et al.*, 2017). The 2007 summer event did not appear to produce significant catchment-wide flooding on the South Tyne, probably due to the localised nature of the storm. However, it is likely that the increasing magnitude and frequency of extreme events shown in the South Tyne peak flow data, is influencing geomorphic processes throughout the catchment.

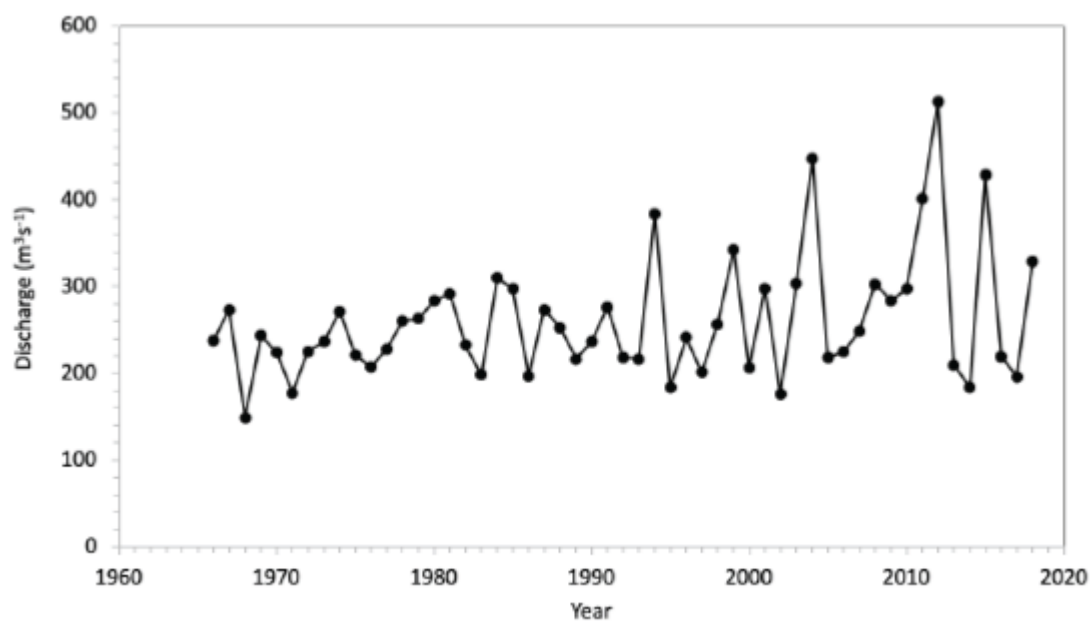


Figure 3 Annual peak flow data for the South Tyne at Featherstone, station 23006 (nrfa.ceh.ac.uk).

Methods

Repeat topographic survey

By monitoring 'geomorphic effectiveness' it is possible to evaluate the response of river systems to floods (Wolman and Miller, 1960; Lisenby *et al.*, 2018). Geomorphic effectiveness is the ability of an event or combination of events to shape or form the landscape. For rivers, metrics of 'cause' most commonly include the 'effective discharge'; the flow that undertakes the most 'geomorphic work' over time, quantified either as the amount of sediment transported (Wolman and Miller, 1960) or 'landform modification' (Wolman and Gerson, 1978). Measuring geomorphic work has traditionally been done through measuring sediment transport, and originally through measuring suspended sediment concentrations (Wolman and Miller, 1960). Milan (2012) however used volumetric changes associated with bedload flux, derived through topographic re-survey, to establish temporal changes in geomorphic work for Thinhope Burn. This approach has also recently been highlighted as a step forward in providing a metric of 'effect'; quantifying the geomorphic effectiveness of events (Lisenby *et al.*, 2018). We continue this methodology herein. Detailed spatially distributed surveys of Thinhope Burn have been conducted on a regular basis since 2003. Between 2003 and 2011 data were collected on four occasions using a Leica System 500 RTK-GPS, and on a further five occasions between 2014 and 2018, using a Topcon GLS2000 Terrestrial LiDAR; where between 6 and 8 scans were merged using tiepoints georeferenced with a Leica System 1200 RTK-GPS in each survey. The early surveys retrieved using RTK-GPS followed a protocol that defined morphological units, capturing the edges of units, and breaks of slope and proven to reduce errors in the DEM (Heritage *et al.*, 2009), and typically had a point density of 1.5 points/m² (Table 1). Our more recent surveys since 2014 using

terrestrial LiDAR, clearly demonstrate the step-change that this instrumentation has had in terms of resolution (Entwistle *et al.* 2018a), with surveys typically collecting 384 points/m². This captured both the immediate geomorphic impacts of the 2007 flood event and recovery in the eleven years following the event. The initial 2003 survey concentrated on a 250 m reach, which was extended to a 500 m reach for all the other surveys. Digital Elevation Models (DEMs) were produced from the point cloud data using a Triangulated Irregular Network (TIN) as the interpolation algorithm (Schwendel *et al.*, 2012), and the data were gridded at 0.1 m. The spatial patterns of erosion and deposition and volumetric changes between surveys were derived from DEM differencing (e.g. Milan *et al.*, 2007). The process of DEM differencing must account for propagated error within each DEM used in the subtraction. Digital Elevation Model error is spatially variable and is largely a function of local topographic variability - with greater error found at breaks of slope such as bank and bar edges (Heritage *et al.*, 2009; Milan *et al.*, 2011; Schwendel and Milan, 2020). Spatial error for each of the DEMs was established using the Milan *et al.* (2011) approach, where full details are given.

Reach-scale hydraulic distribution

We undertook 2D hydrodynamic simulations using CAESAR-Lisflood (Coulthard *et al.*, 2013; Van de Wiel *et al.*, 2007), using different start-state DEMs from every survey conducted on the Thinhope Burn reach, including the pre-flood 2003 DEM, and recovery period DEMs. The model was run with a raster resolution of 1 m. The hydrodynamic model is based on the Lisflood-FP code (Bates and De Roo, 2000); which is a one-dimensional inertial model derived from the full shallow water equations that is applied in the x and y directions to simulate two-dimensional flow over a raster grid (Coulthard *et al.*, 2013).

Discharge between cells is calculated as a function of water surface slope, depth between cells, friction and the discharge between cells from the previous iteration. Although Lisflood FP is primarily used as a flood inundation model, it has also been used to examine channel morphodynamics (e.g. Wong *et al.*, 2015; Entwistle *et al.*, 2018b; Milan *et al.*, 2020). Bates *et al.* (2010) and Neal *et al.* (2012) have demonstrated that the model was capable of simulating flow depths and velocities within 10% of a range of industry full shallow water codes. The flow model should only be applied in sub-critical, gradually varied flow conditions, and consequently simulations over areas of steep terrain with shallow flow depths should be regarded only as a first approximation.

As the aim here was to explore the effect of the different start-state morphologies on the hydraulic patterns and population, the simulations were run in reach-scale hydraulic mode, not allowing for sediment transport or morphological evolution (e.g. Entwistle *et al.*, 2018b). Although spatially distributed roughness can be parametrised in raster-based flood inundation models (Casas *et al.*, 2010), it is common for a uniform roughness coefficient to be applied to the floodplain and treat it as the key calibration parameter (Bates and De Roo 2000; Horritt and Bates 2001a,b, 2002). Skinner *et al.* (2018) identify the Manning's n roughness coefficient as being a highly influential factor on model output, and advise the use of empirical field measurements where possible. In this study spatially distributed roughness data was not available for the full 15 yr period of the investigation. Here we apply a uniform Manning's n of 0.032 to represent grain roughness effects, calculated using Vischer and Hager's (1998) equation

$$n = \frac{(D_{50})^{1/6}}{21.1} \quad (1)$$

where the D_{50} was based on empirical Wolman (1954) grid measurements of grain size in five units including berms, lobes and bars ($D_{50} = 0.126$ m), sampled after the 2007 flood, with form roughness represented through topographic variability in the DEM. To test the sensitivity of Manning's n , and to validate our use of $n=0.032$, we ran models using the 2004 DEM, and discharge hydrograph peaking at $60 \text{ m}^3\text{s}^{-1}$, equivalent to the 2007 flood peak, with different Manning's n coefficients (0.02, 0.03, 0.04, 0.05, and 0.06). We then compared the water elevation output against empirically-derived trash-line elevations obtained shortly after the 2007 event using RTK-GPS. Overall, the simulated water elevations provided a good match when compared relative to those measured represented by the 1:1 line (Figure 4), particularly in the middle of the reach. There is slight underestimation of water surface elevation for all runs at the head of the reach, and more evident towards the tail of the reach, which may reflect boundary conditions at the inlet and outlet of the model domain. Varying the Manning's n seems to have little effect for most of the reach, apart from the tail end of the reach, again possibly due to boundary effects induced by valley narrowing in this region. In the lowest 80 m of the study reach, the width between the valley edge and the 2nd terrace reduced by half, from approximately 30 m to 15 m (see sections x and y on the 2006 image in Figure 2). It has previously been found that LISFLOOD-FP is relatively insensitive to roughness specification when considering it's use on floodplains (Horritt and Bates, 2002). Yu and Coulthard (2015), using the FloodMap-HydroInundation2D model, have further shown output to be relatively insensitive to Manning's n roughness.

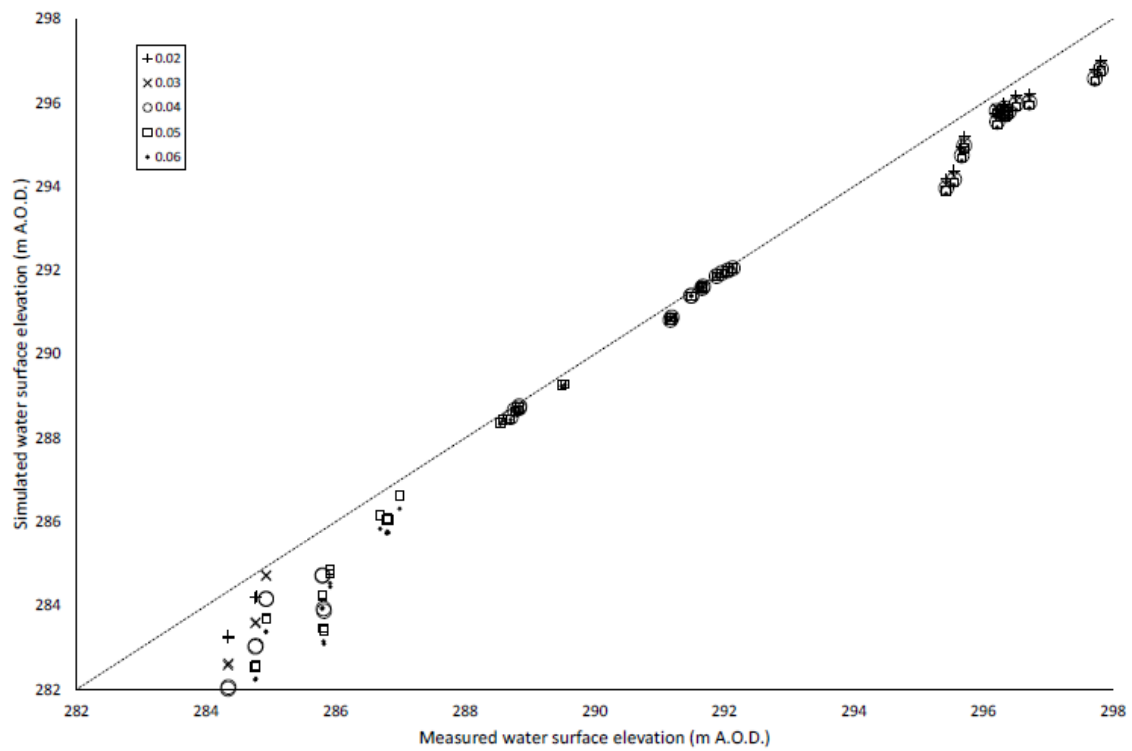


Figure 4 Validation and sensitivity analysis for the Manning's n coefficient.

Temporal changes in bed grain size were not available for the full 15 yr duration of study. However, grain roughness was assessed for the reach as a whole through a spatial analysis of the point cloud data for the five surveys between 2014 and 2018, following procedures outlined in Heritage and Milan (2009). Grain roughness was extracted through determination of twice the local standard deviation ($2\sigma_z$) of all the elevations in a 0.5 m radius moving window over the data cloud. $2\sigma_z$ values were then designated to each node on a 10 cm regular grid, where the elevation is equivalent to the grain roughness height. Table 2 shows reach-average grain roughness derived from this approach and compares this to the Wolman grid measurements taken in 2007. It can be seen that there is little change in reach-average D_{50} . Due to the relative insensitivity of model output and the negligible temporal changes in grain roughness, overall it can be concluded that our global use of $n=0.032$ represents grain roughness effectively in the model.

Shear stress derivation

Lisenby *et al.* (2018) highlight that shear stress has been widely used as a metric of 'cause' when quantifying the action of an event. The depth-average velocity and depth output rasters from the simulations were converted to boundary shear stress (τ_b) using

$$\tau_b = \frac{\rho g V^2 n^2}{y^{\frac{1}{3}}} \text{ (Nm}^2\text{)} \quad (2)$$

where V is depth-averaged velocity, ρ is water density, g is gravitational acceleration, n is the Manning's roughness coefficient, and y is water depth over

each pixel (Thompson and Croke, 2013). We make comparisons of shear stress for the bankfull equivalent flow ($7 \text{ m}^3\text{s}^{-1}$) and for an extreme event; $60 \text{ m}^3\text{s}^{-1}$ equivalent to the 2007 event (Milan, 2012). Comparisons of the low flow ($0.4 \text{ m}^3\text{s}^{-1}$) channel raster outputs from each simulation, also permit comparisons of temporal shifts in planform channel pattern, supplementing topographic change interpretations. This presents a novel departure from traditional assessments of historical planform channel change that often use aerial photographs and historic maps (e.g. Hooke, 2008), that can suffer interpretation issues due to inconsistent water levels.

Results

Morphological evolution

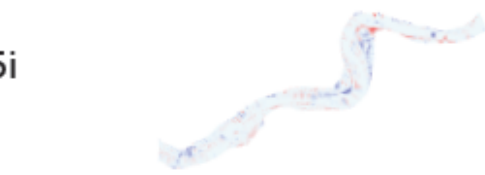
Digital elevation models of difference (DoD) were produced through subtracting successive grids from one another in order to highlight three dimensional changes in the form of spatial patterns of scour and fill (Figure 5). Planform channel pattern evolution is also demonstrated alongside the DoDs, through overlaying successive rasters of the wet channel derived from low flow ($0.4 \text{ m}^3\text{s}^{-1}$) CAESAR-Lisflood simulations. The DoD for 2003-2004 for the downstream 250 m portion of the study reach demonstrates relatively small amounts of change consistent with annual changes expected whilst the system is at steady-state (Table 3). Conversely, the DoD for 2004-2007 for the full 500 m reach shows significant channel changes in response to the flood event. Net deposition of 3077 m^3 , was predominantly found at the head of the reach (Figure 5). This deposition appears to have instigated avulsion of a low amplitude meander, causing the channel to cut across the newly deposited sediment. Significant erosion of berm and terrace

Accepted Article

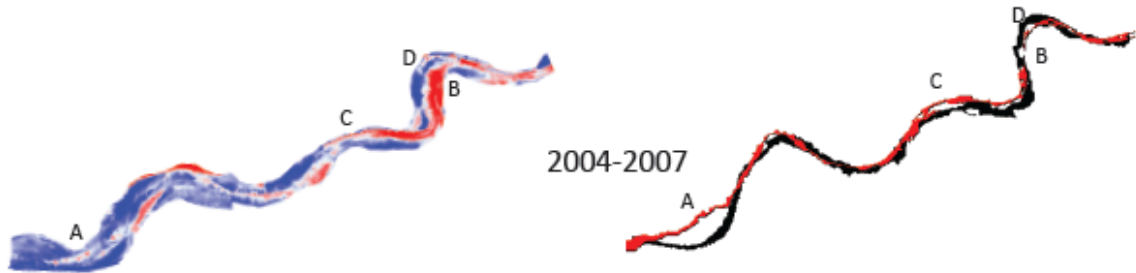
surfaces was also found toward the tail of the study reach (Figure 5B) where a berm, dated by Macklin *et al.* (1992) as being deposited in 1929, was completely remobilised. The former channel running along the outside of the meander became significantly choked with gravel and boulders (Figure 5D), and a new channel towards the right bank was initiated through incision (Figure 5B). There also appears to be a leftward channel shift of the channel in the middle of the reach (Figure 5C).

F5i

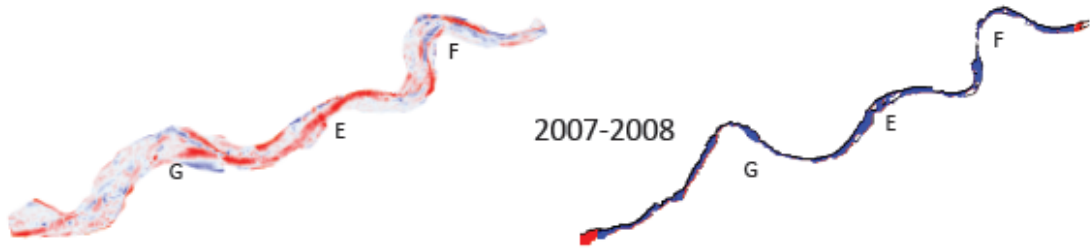
2003-2004



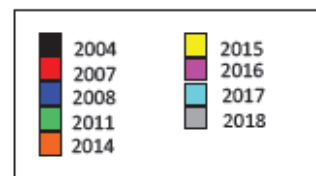
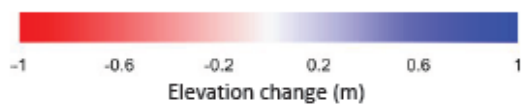
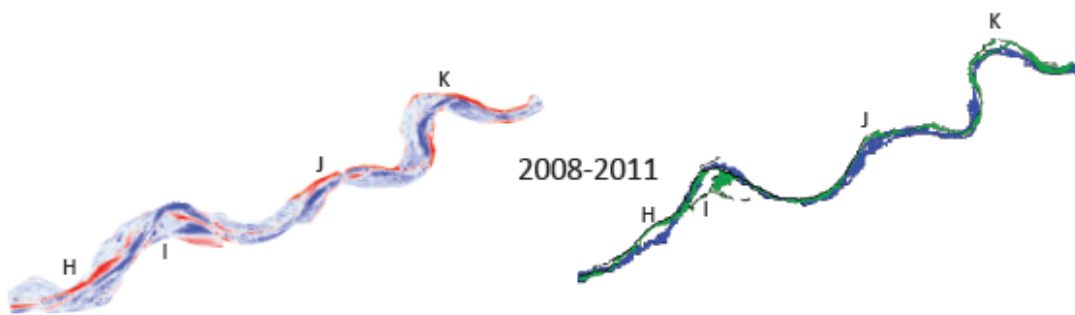
2004-2007



2007-2008



2008-2011



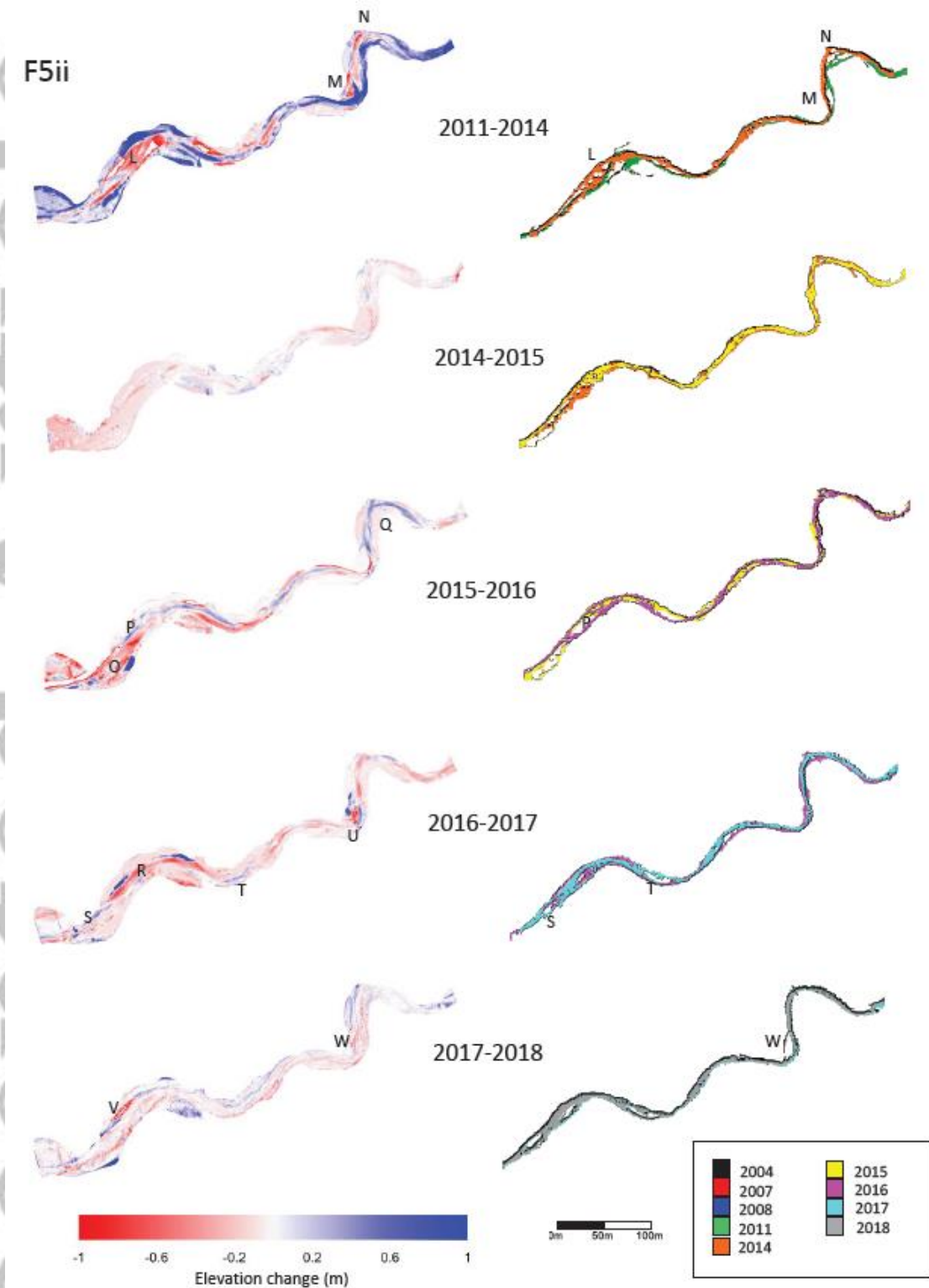


Figure 5 DoDs derived from topographic resurvey. For completeness, the surveys first published in Milan (2012) have also been included in the sequence. Planform channel changes between survey dates are shown on the right of the Figure, using overlays of the low-flow raster outputs from CAESAR-Lisflood.

The DoD for 2007-2008 indicates net erosion of 1838 m³ from the study reach, largely through channel incision. The channel incision identified in the 2004-2007 DoD (Figure 5C) appears to have propagated upstream through the central part of the reach (Figure 5E). Other more localised zones of erosion are evident, for example, further erosion into a terrace toward the tail of the reach and anabranch scour around a new mid-channel bar (Figure 5F). A new mid-channel bar appears to have emerged toward the head of the reach, also as a result of anabranch scour (Figure 5G). The low flow planform channel pattern however appears to remain stable. Large areas of deposition resulting from the 2007 event, on channel margins and former floodplain, remain relatively unchanged.

The DoD for 2008-2011, nearly four years after the event, still suggests that large volumes of sediment are moving through the system; however, the net change is much smaller with overall deposition of 622 m³. Much of the valley floor that was activated by the event was yet to become stabilised with vegetation, resulting in large quantities of material available for transport on the valley floor. At the head of the reach a new avulsion is evident with a planform channel shift to the left, accompanied with incision (Figure 5H). Slightly further downstream deposition in the meander on the left bank appears to be associated with bifurcation around a new mid channel bar with fresh anabranch scour either side (Figure 5I). In the central part of the reach, the channel shows a further slight shift to the left, accompanied with bank and bed erosion (Figure 5J). Toward the tail of the reach, point bars are developing around the edge of the berms. This appears to have caused the channel to shift toward the adjacent terraces, causing undercutting supported through field observation (Figure 5K). This was accompanied with slope failure in this zone, possibly relating to the cold 2010-2011 winter. the head of

the reach the channel has shifted slightly further leftwards, has widened and is multithread in pattern (Figure 5L). There also appears to be channel shift inwards towards the left bank (Figure 5M), associated with full reoccupation of the outside bend of the downstream-most meander (Figure 5N). The channel in this part of the reach has returned to a single-thread pattern. Planform adjustments after 2014, do not appear to be so significant. However, the white/clear patches seen on the low flow channel maps, are indicative of mid-channel bar features, further supporting the notion that the channel has not returned to a stable single-thread pattern, and shows some evidence of a wandering planform in places. Mid-channel bar features are also evident on the aerial images, for 2012, 2017 and 2018 (Figure 2). Much more subtle adjustments took place between 2014 and 2015, with a net change of 16 m³ of deposition. However, greater volumetric changes took place between 2015 and 2016, with net erosion of 396 m³. Most erosion took place towards the head of the reach along the middle of the channel (Figure 5O). Slightly further downstream towards the left bank, deposition has led to the development of a series of mid-channel bars (Figure 5P). Most deposition however, appeared to take place towards the tail of the reach (Figure 5Q). Although there were no major changes to the channel planform, the vertical adjustments influenced the long profile of the channel (Milan and Schwendel, 2019). Between 2016 and 2017 the reach remained vertically active, with 213 m³ of net erosion. Most of this erosion appears to be concentrated along the thalweg, most notably in the upstream end of the reach (Figure 5R). Some areas of blue on the DoD (e.g. Figure 5S, T) appear to be associated with accretion on mid channel bars, also evident on the low flow planform map. There is also evidence of a small avulsion channel on the inside of a berm (Figure 5U), however this does not appear active at low flow. Although erosion and deposition volumes are

substantially less compared with the first seven years following the 2007 flood, the 2017-2018 DoD still evidences notable sediment redistribution, with net deposition of 164 m^3 . There was notable incision in a left bank anabranch to a mid-channel bar (Figure 5V) and return to a single channel planform at the next bend downstream. The avulsion on the inside of the berm, evident in 2017 (Figure 5U), appears to have incised further, now allowing flow to occupy this new channel at low flow (Figure 5W). Despite the substantial net erosion directly after 2007 and the lesser erosion between 2015 and 2017 the cumulative sediment budget for the reach over the study period is still positive with deposition of $>3000 \text{ m}^3$.

Shear stress distribution and population

Shear stress rasters produced using outputs from the CAESAR-Lisflood simulations using different start-state DEMs are shown for the approximate bankfull equivalent flow $7 \text{ m}^3\text{s}^{-1}$ and for an extreme event equivalent to the estimated discharge of the 2007 flood of $60 \text{ m}^3\text{s}^{-1}$ (Figure 6). For the bankfull scenario, shear stress values tend not to exceed 250 Nm^{-2} , whereas shear stresses of up to 800 Nm^{-2} are experienced in the extreme event scenario. The diversity in spatial patterns of shear stress are most evident for the extreme event scenario, with highest shear stresses found along the thalweg, as well as the exit of the reach; a region where flow is constricted by the valley margins (see Figure 2). Lowest shear stress values are seen where flow has spilled on to the floodplain; a feature most strongly evident for the 2004, 2007 and 2008 simulations.

F6

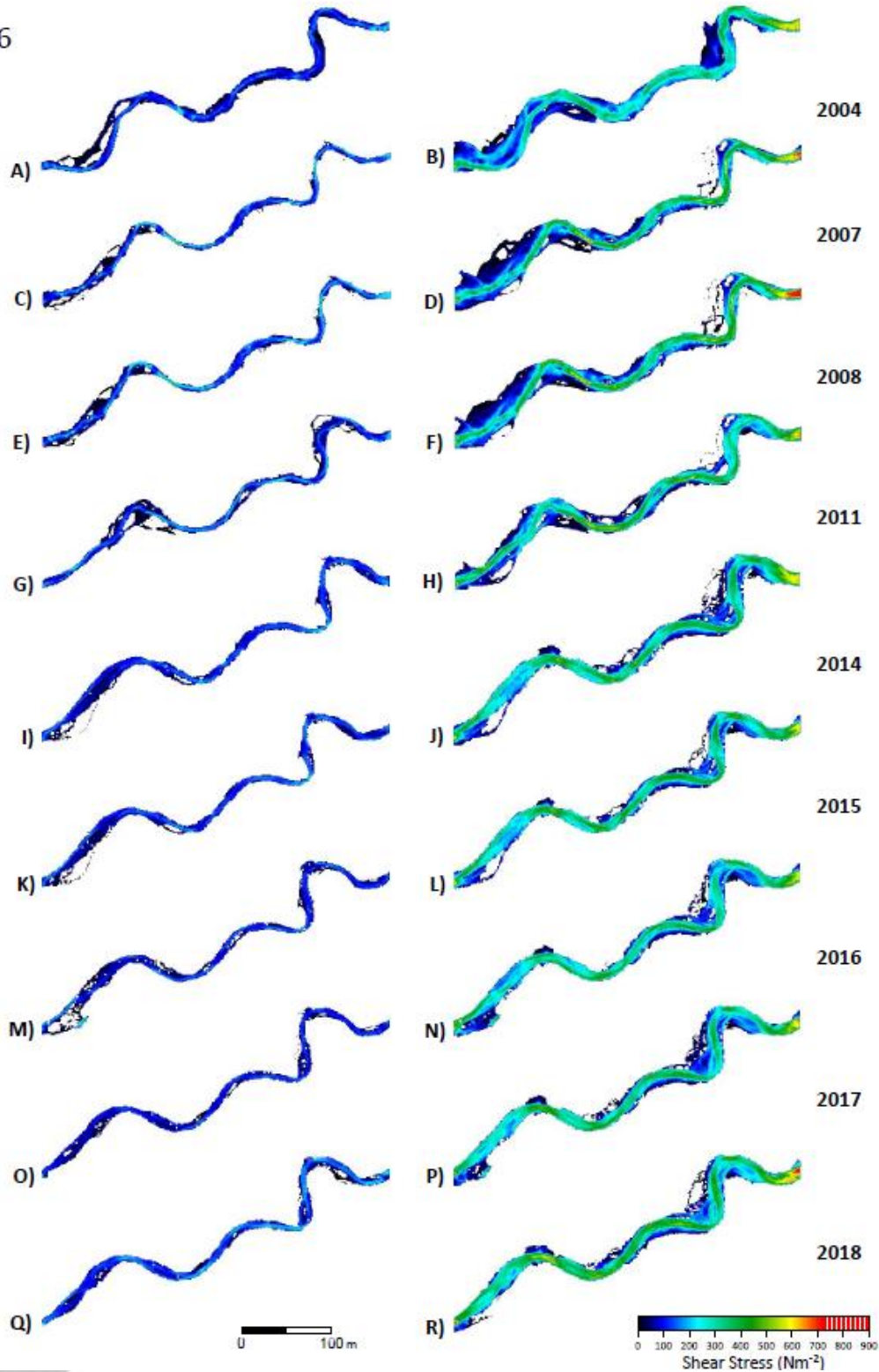


Figure 6 Shear stress raster outputs from CAESAR-Lisflood runs. Each run used a different start-state DEM derived from the temporal topographic re-surveys. Outputs are shown for A) the bankfull equivalent flow ($7 \text{ m}^3\text{s}^{-1}$), and B) an extreme flow equivalent to the 2007 event ($60 \text{ m}^3\text{s}^{-1}$).

The raster outputs shown in Figure 6 were interrogated further through comparing the population distribution of shear stress values for every pixel in every raster (Figure 7). Differences in the shear stress population distributions are driven by changes in the reach morphology, with shifts in shear stress representing changes in bed slope and hydraulic radius, which in turn inform on system stability and sediment transport potential. A general feature of the curves is bimodality shown particularly for the bankfull runs (Figure 7A), and to a lesser extent the extreme event scenario (Figure 7B), where distinct shear stress ranges appear to dominate. To help visualise this, modal shear stress categories (25 to 75 Nm^{-2} , 130 to 180 Nm^{-2} for the bankfull scenario and 25 to 75 Nm^{-2} and $>400 \text{ Nm}^{-2}$ for the extreme event scenario) are highlighted as maps, derived from CAESAR-Lisflood raster outputs, in Figure 8. Figure 8A shows 25 to 75 Nm^{-2} , 130 to 180 Nm^{-2} categories only highlighted as black and blue areas respectively, whilst Figure 8B shows 25 to 75 Nm^{-2} and $>400 \text{ Nm}^{-2}$ only shown as black and red areas respectively. For the bankfull flow 2004 simulation (Figure 7A), a bimodal curve is seen with a modal shear stress in the region of 50 Nm^{-2} . It is the channel margins and banks that appear to be the areas where this primary modal shear stress is concentrated, shown as the black areas on Figure 8A, also evident for 2007, 2008, and 2011 simulations. Although the primary modal shear stress values remain in the region of 50 Nm^{-2} up to 2011, the far right of these curves all plot to the right of the 2004 curve, indicating the presence of much higher shear stress values in the population. Some of the more recent curves (2014, 2017 and 2018) suggest higher modal shear stress values in the region of 150 Nm^{-2} , with the 2015 curve showing a lower modal value of 100 Nm^{-2} , and 2016 reverting back to a modal value of 50 Nm^{-2} . Areas of the bed experiencing concentration of this second mode, are shown as the blue areas in Figure 8A. These areas are concentrated

along the thalweg, and appear to show some organisation, tending to be located towards the outside meanders. It is noteworthy that all post 2004 curves (Figure 7A), with the exception of 2017, have greater proportions of their shear stress population exceeding 200 Nm^{-2} , indicating more energetic systems at the bankfull discharge.

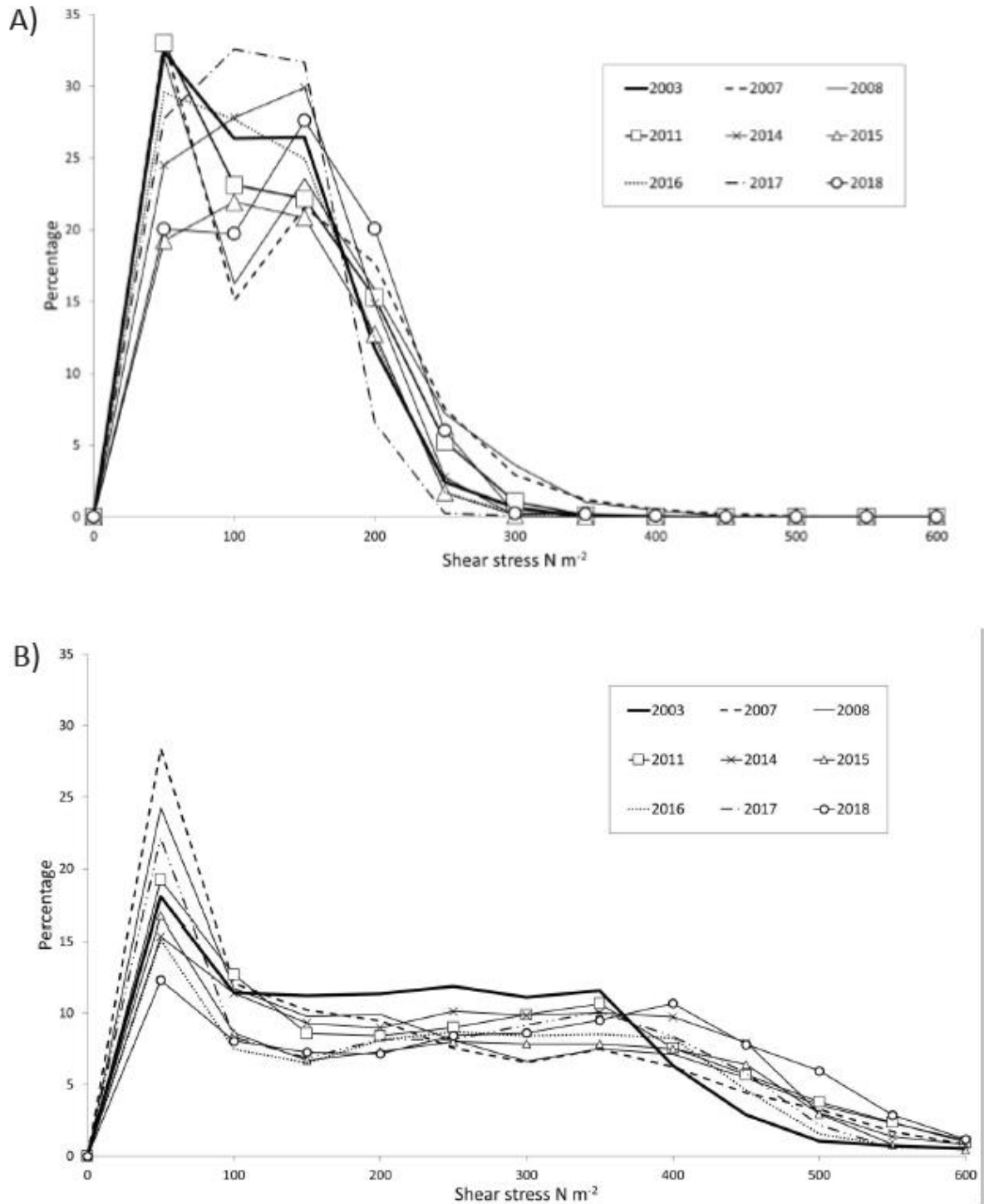


Figure 7 Population distribution of shear stress using values from each pixel in the rasters derived from the CAESAR-Lisflood outputs shown in Figure 6, for A) the bankfull equivalent flow ($7 m^3 s^{-1}$), and B) an extreme flow equivalent to the 2007 event ($60 m^3 s^{-1}$). Flow hydrographs for these flow peaks were run using nine different starter DEMs representing pre 2007 flood DEM (2004), and then using post flood DEMs between 2007 and 2018.

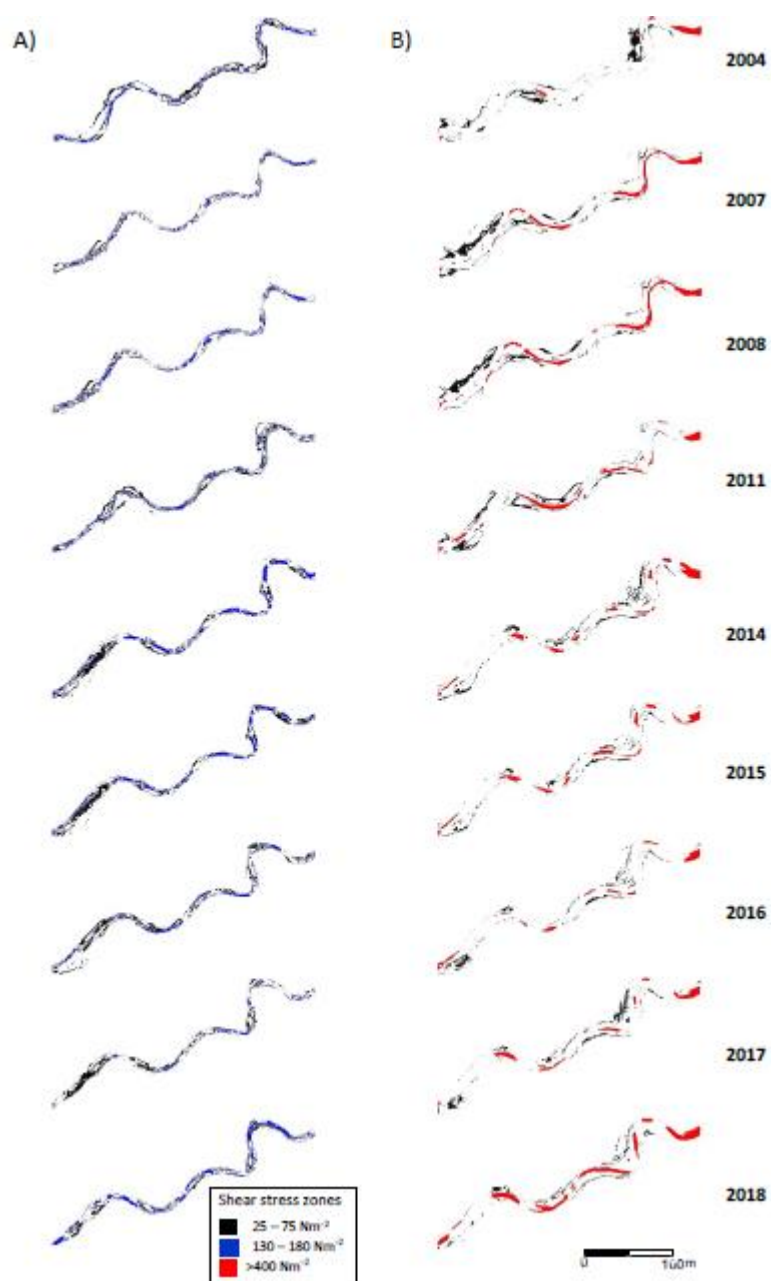


Figure 8 Spatial patterns of modal shear stress A) 25 to 75 Nm^{-2} , 130 to 180 Nm^{-2} for the bankfull scenario and B) 25 to 75 Nm^{-2} and >400 Nm^{-2} for the extreme event scenario.

For the extreme event scenario (Figure 7B), the modal shear stress for all curves is around 50 Nm^{-2} , however there is a much wider spread of values with shear stresses up to in excess of 400 Nm^{-2} . The modal shear stress appears to be concentrated at the channel margins and banks, as well as on the floodplain surface, shown as the black areas in Figure 8B. For the 2004 simulation there is a notable black area on the floodplain surface on the inside of a meander towards the tail of the reach, and for the 2007 and 2008 simulations large areas are evident on the left-bank floodplain surface at the head of the reach. These three simulations possibly indicate the potential for greater geomorphic work on the floodplain in comparison to the later simulations, where the black areas tend not to be so large in their spatial extent. Post 2007 flood curves tend to have a lower proportion of mid-range shear stresses ($100\text{--}400 \text{ Nm}^{-2}$), compared with the 2004 curve, however they have a much larger proportion of their populations in excess of 400 Nm^{-2} (Figure 7B). These high energy areas, indicated as red zones on Figure 8B, are not so widespread when viewing the 2004 simulation. However, these become much more widespread in the simulations that are run using the post-2007 flood DEM's, particularly for the 2007 and 2008 runs. There is a slight reduction in the areal extent of $>400 \text{ Nm}^{-2}$ areas shown in the 2011, 2014, 2015, 2016 and 2017 simulations, however an increase in the areal coverage is shown again in the 2018 simulation. When viewing the shear stress curves in Figure 7B, there is a suggestion of some recovery, with the 2016 and 2017 curves showing a reduction in the proportion of very high shear stress values, and an increase in the mid-range shear stresses. The 2018 data, reverts back and actually shows the greatest proportion of $>450 \text{ Nm}^{-2}$ values out of all the simulations. However, there is never a return to the much more limited spatial extent of areas $>400 \text{ Nm}^{-2}$ shown in the 2004 run.

Overall, this analysis suggests that the morphological modifications made by the 2007 flood result in higher shear stress values. The first mode in the frequency distributions (Figure 7) is associated with limited flow depth on the floodplain and channel margins while the frequency of higher shear stress is conditioned by the channel morphology (e.g. aggradation and incision) and thus the pronunciation of the second mode is more variable at bankfull and absent when the entire valley floor is flooded. The increased shear stress values are not thought to be linked to changes in reach slope, as average slope remained between 3.0 and 3.5% throughout the study period. It is more likely to reflect greater vertical variations on the bed (increased form roughness), that produce deeper areas and greater local depths at high flow; and it is these areas that experience the higher shear stresses.

Reach-average gross temporal trends in shear stress

A further assessment of gross temporal trends in shear stress may be examined through looking at the temporal change in reach-average shear stress, calculated by taking the reach-wide sum of shear stress for each raster and normalising the totals by the number of grid cells involved (Figure 9). For the bankfull scenario ($7 \text{ m}^3\text{s}^{-1}$) an initial rise in shear stress is seen using the 2007 (post flood) DEM and for the 2008 CAESAR-Lisflood simulation, that may relate to areas of scour along the thalweg creating deeper zones. The post-2008 trend appears to be one of a reduction in the shear stress until 2017, which could be argued to represent recovery. This seems to relate to a trend of net deposition which is evident between 2008 and 2015. The gradual erosion of the material deposited in the channel from 2016 eventually results in the higher shear stress

in 2018; exemplifying the increased sensitivity of the reach. Although there was net deposition in 2018 this was concentrated on banks and overbank areas, while erosion was spatially dominant in the channel (Figure 5).

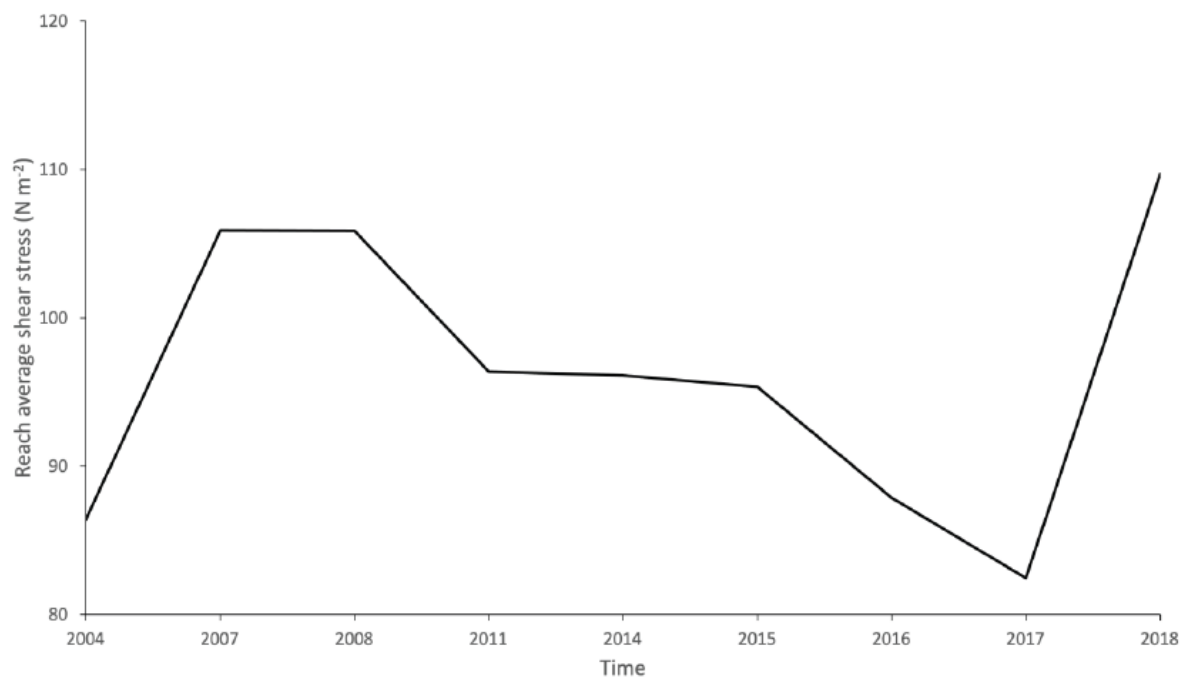


Figure 9 Temporal trends in reach average shear stress total for the bankfull scenario ($7 \text{ m}^3\text{s}^{-1}$).

Discussion

Consideration of conceptual frameworks

System behaviour for Thinhope Burn is conceptualised in Figure 10. Pre-flood channel adjustment fluctuates within limiting thresholds (*sensu* Schumm, 1979) controlled by the key extrinsic factor: climatic regime. We argue that the pre-2007 channel reflected the channel state controlled by the drier climatic phase prior to 1993 (Figure 2). What we see in the period between 1993 and 2007 is a system that moves closer to exceeding the limiting thresholds, and it was the 2007 event that pushed the system over the edge; the 'tipping-point', whereby the magnitude and duration of the rainfall event triggered activation of the full sediment system, instigating major geomorphic changes (Phillips, 2014). This resulted in an order of magnitude increase in geomorphic work as demonstrated in the sediment transport volumes seen (Figure 10A). There appears to be a relaxation phase evident between 2008 and 2014 (highlighted by the blue box in Figure 10A), whereby there is still significant re-working of bedload. Topographic re-survey does suggest a reduction in geomorphic work in the eleven years following the event. However, there does not appear to be a return back to the previous system state and even small flood events are predicted to produce considerable shear stress (Figure 7A and 8). Erosion and deposition still exceed pre-flood volumes, and planform geomorphic evidence (Figure 5) still shows an over-wide wandering channel with mid-channel bars as opposed to a stable single-thread channel. Our 2D hydrodynamic modelling (Figures 6, 7, 8, 9) also suggests that morphological adjustments since the 2007 flood, support a more energetic system, with a greater proportion of the bed experiencing higher shear stresses and thus capable of transporting more bedload in comparison to the pre-2007 condition. Although there is a suggestion of recovery shown with decreasing shear

stresses for the bankfull simulations (Figure 9), a return to high shear stresses in 2018 seems to support the notion of increased sensitivity in the reach (*sensu* Brunnsden and Thornes, 1979; Downs and Gregory, 2003; Fryirs, 2017). Direct comparison between simulated shear stress and morphological changes are complicated because the effect of unknown flood magnitudes since 2007 on the surveyed surfaces cannot be assessed. Nevertheless, the shear stress simulations provide a process-informed link to the observed topographies. We argue therefore that the post-2007 channel is one that is adjusted to the current wet phase in UK climate, fluctuating around a new steady state condition, and that in the foreseeable future the channel will remain a wandering channel with mobile bedload.

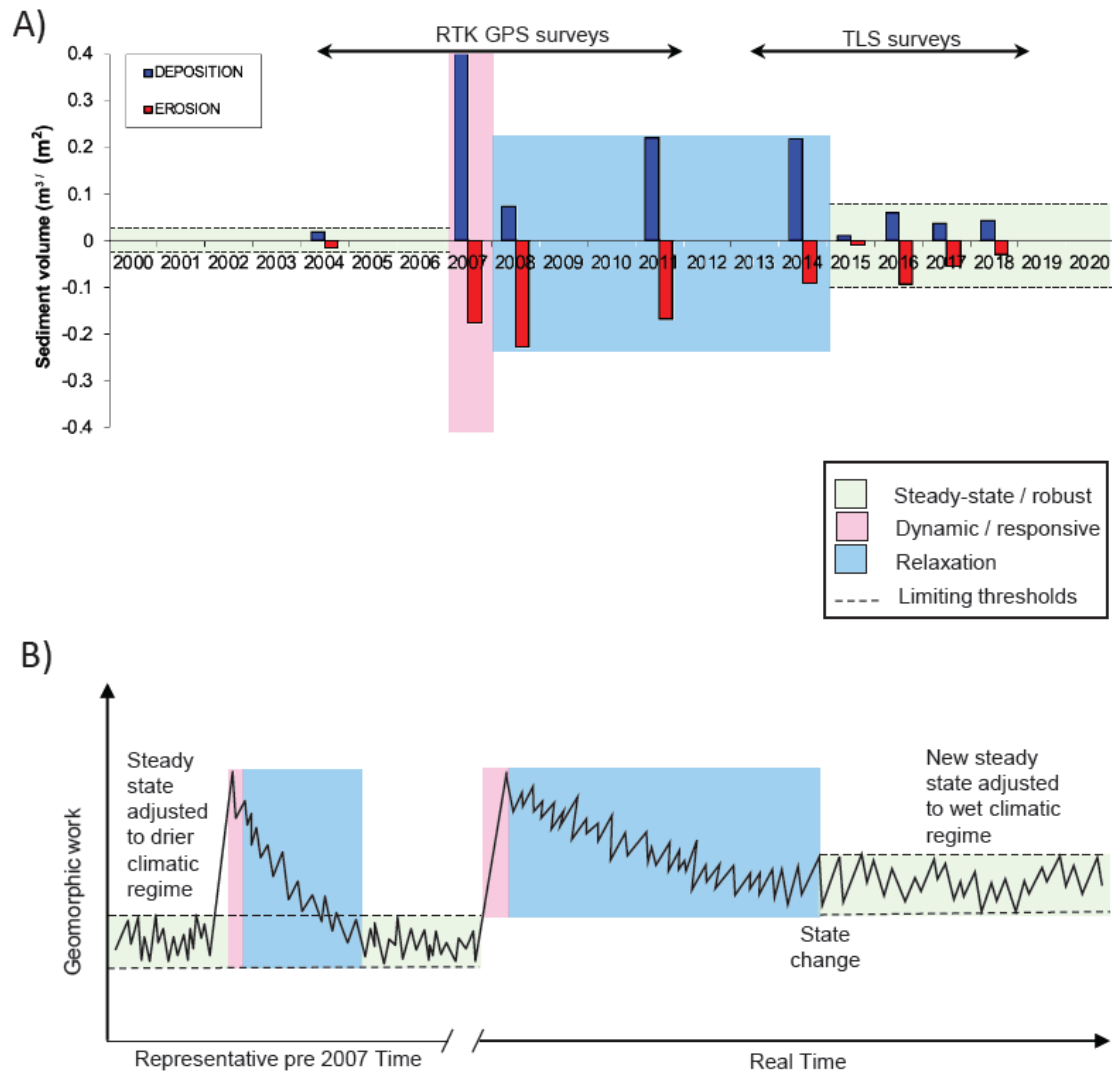
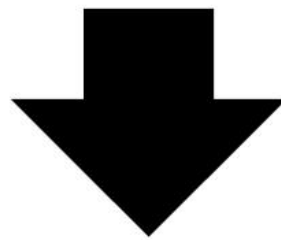
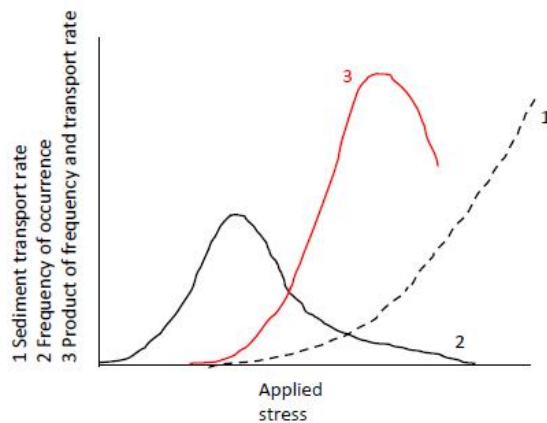


Figure 10 Conceptual framework for understanding upland channel response to climate-change driven changes in flood magnitude and frequency: A) Geomorphic work as defined by empirically derived erosion and deposition volumes for the lower 250-m portion of the study reach during steady-state and dynamic equilibrium: B) conceptual model of longer-term response of Thinhope Burn to flood events.

At present the system appears much more 'responsive' and 'sensitive' to change (*sensu* Brunsden and Thornes, 1979; Brunsden, 2001) and this sensitivity seems to be driven by several different controls. The current system state is not only subject to the effects of a wetter climatic regime inducing higher and more frequent flood peaks (e.g. Dadson *et al.*, 2017), but due to vegetation loss from the valley floor, the availability of new sediment sources, enhanced system connectivity, and a more frequently disrupted and unstructured channel bed (Dietrich *et al.*, 1989), lower magnitude events are able to undertake comparatively more geomorphic work (Figure 11).

A)



B)

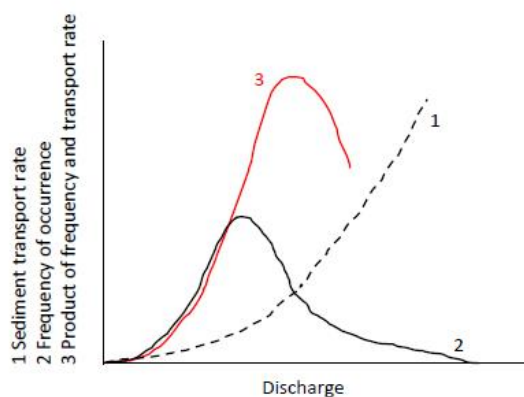


Figure 11 A) Heritage and Milan's (2004) relations between rate of transport, applied stress, and frequency of stress application based on channel response in dryland bedrock channels. Curve 3 (Geomorphic work) shifts to the right, compared with the original Wolman and Miller (1960) diagram, to represent mobilisation of the gravel/boulder load. Robust systems require rare large events to transport large sediment load, due to increased strength of vegetated floodplain and armoured bed. B) Wolman and Miller's (1960) relations between rate of transport, applied stress, and frequency of stress application for temperate alluvial channels. Once system state changed, the sensitive system responds more easily to lower magnitude flows, transporting much more sediment load for an equivalent discharge when compared with the robust system.

We contend that prior to the 2007 flood, that Thinhope behaved in a similar manner to the conceptual model proposed by Heritage and Milan (2004) for coarse bedded upland channels (Figure 10A); a modified version of Wolman and Millers (1960) original model for temperate river systems (Figure 10B), where the mass of transported sediment (curve 1) is a power function of discharge, whilst the discharge frequency (curve 2) is positively skewed. The product of the two curves (curve 3), the maximum geomorphic work spent over a given period, should have a distribution that peaks at the most 'effective' or 'dominant' discharge or applied stress. Heritage and Milan (2004) contended that Wolman and Millers (1960) original diagram designed for suspended sediment loads, may not be applicable to gravel bed river channels, where it is the higher magnitude floods that were the 'effective' geomorphic agents, as these have the ability to mobilise both 'Phase 1 -sand' and 'Phase 2-gravel' loads, and hence change channel form. We further propose that when river channels are in their robust state that the maximum geomorphic work (curve 3) needs to be positioned further to the right in comparison to Wolman and Miller (1960), in order to tip those thresholds required to tear up floodplains and their vegetation, and mobilise paleo berms, lobes and splays perched at higher elevations on terrace surfaces. Once these morphological units are disrupted by an extreme event, sediment stores on the valley floor are released into the system resulting in very high sediment transport rates not only during the event but also by the smaller floods that follow as the system attempts to recover. Hence, the amount of work undertaken by the rare large flood and the smaller floods that follow during the recovery period exceeds the cumulative work undertaken by floods whilst the system is at steady-state.

Prior to the 2007 flood on Thinhope Burn, the channel was a narrow single-thread sinuous channel, with a stable vegetated floodplain with well-established grasses, heather (*Calluna vulgaris*), and bracken (*Pteridium aquilinum*) in summer (Figure 11A). The system in this state could be regarded as 'robust' in character (Brunsden and Thornes, 1979). Soil and vegetation establishment increases the strength of the floodplain unit (Abernethy and Rutherford, 2001) and less frequent bedload transport results in enhanced armouring and structural enhancement of the in-channel bed surface; both factors that increase system robustness. The 2007 flood ripped away much of the floodplain surface removing vegetation, and fully mobilising the bed, widening the channel and promoting a wandering channel planform (Figure 2; 11B). Now that Thinhope Burn has been 'sensitised' by the 2007 flood, we postulate that its behaviour seems to be more akin to the original Wolman and Miller (1960) model (Figure 11B), where higher frequency lower magnitude flows, perhaps equating to the bankfull condition (Andrews, 1980) may be undertaking more cumulative geomorphic work in comparison to the rare extreme event.

System connectivity

Sediment connectivity within the Thinhope Burn catchment is also highly significant in controlling the amount of geomorphic work undertaken (Fryirs, 2013). Key sediment stores are held in paleo berms, lobes and splays perched on several terraces, at different elevations from the contemporary channel. The terraces themselves also provide sediment stores, and further sources are derived from till and bedrock in the second order tributaries upstream. Some slope-channel coupling zones do exist that are connected to the channel, and it is likely that these provide enhanced supply conditioned by weather conditions;

not just rainfall but freeze-thaw action during the winter can help induce slope failures. This was thought to supply sediment to the downstream part of the study reach following the 2010-11 winter. Under a drier climatic phase, we suggest that flood peaks rarely achieve the water elevations needed to tap into many of the stores held in the third order part of the system, nor do they have the energy to mobilise some of the coarse boulder deposits held within them.

Implications for future flood risk management

The hydro-geomorphic response of upland headwater streams to intense storm events is clearly a concern not only for the direct impact on human life and damage to infrastructure (Borga *et al.*, 2011; Munich, 2018; The International Disaster Database, 2021), but also for management sediment and longer-term flood risk in downstream areas (Radice *et al.*, 2013; Marchi *et al.*, 2010). Regional forecasts derived from Global Climate models indicate that upland areas of the UK are amongst the most susceptible areas to winter rainfall increases and extreme summer events (Dadson *et al.*, 2017; Murphy *et al.*, 2020). Not only will this increase water volumes delivered to the channel network further downstream, but may also cause significant increases in bedload mobilisation, with potential morphological changes cascading downstream through river catchments, and well documented in other parts of Europe (Lucia *et al.*, 2015; Surian *et al.* 2016; Ruiz-Villanueva *et al.*, 2018; Scorpio *et al.*, 2018). The impacts of climate change on upland geomorphic systems are already clear. For example, in the Storm Desmond floods of December 2015, the local flooding at Glenridding, Cumbria, UK, was strongly influenced by reduced channel capacity linked to sediment delivery (McCall and Webb, 2016; Heritage *et al.*, 2019). In addition, the same event activated torrents, resulting in delivery of sediment to major road routes,

causing them to be closed (Warburton *et al.*, 2016). The effects of a wetter climatic regime on our upland catchments could be bringing some headwater catchments closer to tipping-points, whereby much greater sediment volumes are activated from slopes and floodplains, transported and delivered downstream. In addition, once sediment system activation takes place, a new sediment transport regime is established that is adjusted to the new wetter climatic regime, and hence these catchments are unlikely to recover. In the South Tyne catchment annual peak flows have clearly increased since the 1990s (Figure 2), and although evidence is not widespread across the whole of the South Tyne, Thinhope Burn provides an example of a catchment that has become severely impacted and one that does not show recovery even 11 years after the original flood.

It is essential that upland flood risk management in the future builds-in key geomorphic concepts including; geomorphic effectiveness, thresholds, sensitivity, connectivity and recovery (Fryirs, 2013; 2015; Lisenby *et al.*, 2018). At a National scale in the UK, flood risk managers need to understand which catchments are most at risk to sediment system activation. Once identified, the potential impacts of sediment system activation need to be simulated in order to predict the likely implications for long-term flood risk in a wetter climatic regime. This will then facilitate focussed flood risk management strategies and possibly permit tailored approaches to flood risk management grounded in geomorphic principles. This could be achieved by adopting a modified Fluvial Audit (Sear and Newson, 2003), approach utilising GIS and field-based assessment by trained geomorphologists, and subsequent morphodynamic modelling of those catchments identified as being close to tipping points.

Conclusions

We argue that the current wet phase in UK climate could be pushing some upland catchments closer to tipping points, whereby their sediment systems become activated, with the potential to dramatically increase sediment delivery downstream and enhancing flood risk. The example presented in this paper for a 500 m reach of Thinhope Burn, demonstrates that 11 years following an extreme summer flood in 2007, the valley floor of still remains very active and although erosion and deposition volumes from year to year have shown a reduction, the reach still has not fully recovered to its pre-2007 condition. Hydraulic outputs ran on different start state DEMs, derived from near-annual re-surveys, demonstrate greater hydraulic energy on the post 2007 flood runs. We argue that this demonstrates a switch to a more energetic system state, adjusted to the current wetter climatic regime experienced in the South Tyne catchment as a whole, and which is evidenced in the peak flow record. This indicates that there is still the potential for enhanced bedload transport and morphological adjustment within the reach. We further argue that catchments that are impacted like Thinhope Burn may not recover under the wet climatic phase currently being experienced, and such systems will continue to deliver large volumes of sediment further down river catchments, providing new challenges for flood risk management into the future.

Data Availability Statement

The data that support the findings of this study are available on request from the lead author.

Conflicts of interest

The authors declare no conflicts of interest.

References

- Abernethy, B., Rutherford, I.D. 2001. The distribution and strength of riparian tree roots in relation to riverbank reinforcement. *Hydrological Processes* **15**: 63-79.
- Allamano, P., Claps, P., Laio, F. 2009. Global warming increases flood risk in mountainous areas. *Geophysical Research Letters* **36**(24).
- Andrews, E.D. 1980. Effective and bankfull discharges of streams in the Yampa river basin, Colorado and Wyoming. *Journal of Hydrology*: **46**, 311–330.
- Barrera-Escoda, A., Llasat, M.C., 2015. Evolving flood patterns in a Mediterranean region (1301–2012) and climatic factors—the case of Catalonia. *Hydrology and Earth System Sciences* **19**(1): 465-483.
- Bates, P.D., De Roo, A.P.J. 2000. A simple raster-based model for flood inundation simulation. *Journal of Hydrology*, **236**(1–2): 54–77.
[https://doi.org/10.1016/S0022-1694\(00\)00278-X](https://doi.org/10.1016/S0022-1694(00)00278-X)
- Bates, P., Horritt, M., Fretwell, J. 2010. A simple inertial formulation of the shallow water equations for efficient two-dimensional flood inundation modelling. *Journal of Hydrology* **387**: 33–45.
- Beniston, M. Stoffel, M., Hill, M. 2011. Impacts of climatic change on water and natural hazards in the Alps: Can current water governance cope with future

challenges? Examples from the European “ACQWA” project. *Environmental Science & Policy* **14**: 734-743.

Borga M Anagnostou EN Blöschl G and Creutin JD (2011) Flash flood forecasting, warning and risk management: the HYDRATE project. *Environmental Science & Policy* **14**: 834-844.

Brierley, G., Fryirs, K. 2009. Don't fight the site: three geomorphic considerations in catchment-scale river rehabilitation planning. *Environmental Management* **43**(6): 1201-1218.

Brunsdon, D. 2001. A critical assessment of the sensitivity concept in geomorphology. *Catena* 42: 99-123.

Brunsdon, D., Thornes, J.B. 1979. Landscape sensitivity and change. *Transactions of the Institute of British Geographers New Series* **4**: 463–484.

Carling, P.A. 1986. The Noon Hill flash floods; July 17th 1983. Hydrological and geomorphological aspects of a major formative event in an upland landscape. *Transactions of the Institute of British Geographers* **11**: 105–118.

Casas, A., Lane, S.N., Yu, D., Benito, G. 2010. A method for parameterising roughness and topographic sub-grid scale effects in hydraulic modelling from LiDAR data. *Hydrology and Earth System Sciences* **14**: 1567-1579.

Coulthard, T. J., Neal, J. C., Bates, P. D., Ramirez, J., Almeida, G. A. M., Hancock, G. R. 2013. Integrating the LISFLOOD-FP 2D hydrodynamic model with the CAESAR model: Implications for modelling landscape evolution. *Earth Surface Processes and Landforms* **38**: 1897–1906.

Dadson, S.J.; Hall, J.W. Murgatroyd, A. Acreman, M., Bates, P.; Beven, K.

O'Connell, E. A. 2017. Restatement of the natural science evidence concerning catchment-based 'natural' flood management in the UK. *Proceedings of the Royal Society A. Mathematics Physics and Engineering Sciences*, **473**.

- Dietrich, W.E., Kirchner, J.W., Ikeda, H., Iseya, F., 1989. Sediment supply and the development of the coarse surface layer in gravel-bedded rivers. *Nature* **340**: 215-217.
- Downs, P.W. Gregory, K.J. 1993. The sensitivity of river channels in the landscape system. In: Thomas DSG and Allison R (eds) *Landscape Sensitivity*. John Wiley & Sons, New York, pp. 15–30.
- Entwistle, N., Heritage, G., Milan, D., 2018a. Recent remote sensing applications for hydro and morphodynamic monitoring and modelling. *Earth Surface Processes and Landforms* **43**:2283-2291.
- Entwistle, N., Heritage, G., Milan, D. 2018b. Flood energy dissipation in anabranching channels. *River Research and Applications* **34**(7): 709–720.
- Foulds, S.A., Brewer, P.A., Macklin, M.G., Haresign, W., Betson, R.E., Rassner, S.M.E. 2014. Flood-related contamination in catchments affected by historical metal mining: an unexpected and emerging hazard of climate change. *Science of the Total Environment* **476**: 165-180.
- Fryirs, K.A. 2013. (Dis) Connectivity in catchment sediment cascades: a fresh look at the sediment delivery problem. *Earth Surface Processes and Landforms* **38**: 30-46.
- Fryirs, K.A. 2017. River sensitivity: A lost foundation concept in fluvial geomorphology. *Earth Surface Processes and Landforms* **42**: 55-70.
- Fuller, I.C., Large, A.R.G., Charlton, M.E., Heritage, G.L., Milan, D.J. 2003b. Reach-scale sediment transfers: an evaluation of two morphological budgeting approaches. *Earth Surface Processes & Landforms* **28**: 889-903.
- Fuller, I.C., Large, A.R.G., Milan, D.J. 2003a. Quantifying channel development and sediment transfer following chute cut-off in a wandering gravel-bed river. *Geomorphology* **54**: 307-323.

Fuller, I.C., Passmore, D.G., Heritage, G.L., Large, A.R.G., Milan, D.J., Brewer, P.A. 2002. Annual sediment budgets in an unstable gravel bed river: the River Coquet, northern England. In Jones, S., Frostick, L. (eds) *Sediment flux to basins: causes, controls and consequences*, Geological Society of London Special Issue **191**: 115-131.

Groisman PY Knight RW Karl TR Easterling DR Sun B Lawrimore J (2004) Contemporary changes of the hydrological cycle over the contiguous United States: trends. *Journal of Hydrometeorology* **5**: 64–85.

Groisman PY Knight RW Easterling DR Karl TR Hegerl GC Razuvaev VN (2005) Trends in intense precipitation in the climate record. *Journal of Climate* **18**:1326–1350.

Harvey, A.M. 1986. Geomorphic effects of a 100-year storm in the Howgill Fells, northwest England. *Zeitschrift für Geomorphologie* **30**: 71–91.

Harvey, A.M. 2007. Differential recovery from the effects of a 100-year storm: Significance of long-term hillslope–channel coupling; Howgill Fells, northwest England. *Geomorphology*, **84**(3-4):192-208.

Heritage, G.L., Milan, D.J. 2004. A conceptual model of the role of excess energy in the maintenance of a riffle–pool sequence. *Catena* **58**: 235-257.

Heritage, G.L., Entwistle, N. Milan, D.J. 2019. Evidence of non-contiguous flood driven coarse sediment transfer and implications for sediment management. *Proceedings of the 38th IAHR World Congress, Panama, September 1-6 Sept, 2019, Panama City, Panama*, 113-120,

Heritage, G.L., Large, A.R.G. Milan, D.J. in press. *A field guide to British Rivers*. Wiley-Blackwell.

Heritage, G.L., Milan, D.J., 2009. Terrestrial laser scanning of grain roughness in a gravel-bed river. *Geomorphology*: **113**(1-2): 4-11.

- Heritage, G.L., Milan, D.J., G.L., Large, A.R.G., Fuller, I. 2009. Influence of survey strategy and interpolation model upon DEM quality. *Geomorphology* **112**: 334-344.
- Hooke, J.M., 2008. Temporal variations in fluvial processes on an active meandering river over a 20-year period. *Geomorphology* **100**:3-13.
- Horritt MS, Bates PD. 2001a. Effects of spatial resolution on a raster based model of flood flow. *Journal of Hydrology* 253: 239–249.
- Horritt MS, Bates PD. 2001b. Predicting floodplain inundation: raster-based modelling versus the finite-element approach. *Hydrological Processes* 15: 825–842.
- Horritt, M.S., Bates, P.D. 2002. Evaluation of a 1D and 2D numerical models for predicting river flood inundation. *Journal of Hydrology* **268**: 87–99.
- Kleinen, T., Petschel-Held, G. 2007. Integrated assessment of changes in flooding probabilities due to climate change. *Climate Change* **81**: 283–312.
- Lane, S.N., Tayefi, V., Reid, S.C., Yu, D., Hardy, R.J. 2007. Interactions between sediment delivery, channel change, climate change and flood risk in a temperate upland environment. *Earth Surface Processes Landforms* **32**: 429–446.
- Lisenby, P.E., Croke, J., Fryirs, K.A. 2018. Geomorphic effectiveness: a linear concept in a non-linear world. *Earth Surface Processes and Landforms* **43**(1): 4–20.
- López Bustos, A., 1964. Resumen y conclusiones de los estudios sobre avenidas del Valles en 1962. Instituto de Hidrolog.a, Technical Report, Madrid.
- Lucía, A., Comiti, F., Borga, M., Cavalli, M., Marchi, L. 2015. Dynamics of large wood during a flash flood in two mountain catchments. *Natural Hazards and Earth System Sciences* **15**(8): 1741-1755.

- Macklin, M.G., Rumsby, B.T., Heap, M.T. 1992. Flood alluviation and entrenchment: Holocene valley-floor development and transformation in the British uplands. *Geological Society of America Bulletin* **104**: 631–643.
- Marchi, L., Borga, M., Preciso, E., Gaume, E. 2010. Characterisation of selected extreme flash floods in Europe and implications for flood risk management. *Journal of Hydrology* **394**(1-2): 118-133.
- McCall, I., Webb, D. 2016. Glenridding flood investigation report. Environment Agency and Cumbria County Council.
<https://cumbria.gov.uk/elibrary/Content/Internet/536/6181/4255914426.PDF>
- Milan, D.J. 2012. Geomorphic impact and system recovery following an extreme flood in an upland stream: Thinhope Burn, northern England, UK. *Geomorphology* **138**(1): 319-328.
- Milan, D.J., Heritage, G.L., Hetherington, D. 2007. Application of a 3D laser scanner in the assessment of erosion and deposition volumes in a proglacial river. *Earth Surface Processes & Landforms* **32**(11): 1657-1674.
- Milan, D.J., Heritage, G.L., Large, A.R.G., Fuller, I. D. 2011. Filtering spatial error from DEMs; implications for morphological change estimation. *Geomorphology* **125**: 160-171.
- Milan, D.J., Tooth, S., Heritage, G.L. 2020. Topographic, hydraulic and vegetative controls on bar and island development in mixed bedrock-alluvial multichanneled, dryland rivers. *Water Resources Research* **56**.
<https://doi.org/10.1029/2019WR026101>
- Munich, R.E. 2019. Relevant natural loss events worldwide 1980–2018. NatCatSERVICE
- Murphy, J.M., Brown, S.J., Harris G.R. 2020. UKCP Additional Land Products: Probabilistic Projections of Climate Extremes. Met Office, Exeter

<https://www.metoffice.gov.uk/binaries/content/assets/metofficegovuk/pdf/research/ukcp/ukcp-probabilistic-extremes-report.pdf>

Murphy, J.M., Sexton, D.M., Jenkins, G.J., Booth, B.B., Brown, C.C., Clark, R.T., Collins, M., Harris, G.R., Kendon, E.J., Betts, R.A., Brown, S.J. 2009. UK climate projections science report: climate change projections.

Neal, J., Villanueva, I., Wright, N., Willis, T., Fewtrell, T., Bates, P. 2012. How much physical complexity is needed to model flood inundation? *Hydrological Processes* **26**: 2264–2282.

Newson, M. 1980. The geomorphological effectiveness of floods—a contribution stimulated by two recent events in mid-Wales. *Earth Surface Processes* **5**(1): 1–16.

Parry, S., Barker, L., Sefton, C., Hannaford, J., Turner, S., Muchan, K., Matthews, B., Pennington, C. 2021. Briefing Note: Severity of the February 2020 floods -preliminary analysis.

https://nrfa.ceh.ac.uk/sites/default/files/Briefing_Note_V6.pdf

Phillips, J.D. 2014. State transitions in geomorphic responses to environmental change. *Geomorphology* 204: 208–216.

Radice, A., Rosatti, G., Ballio, F., Franzetti, S., Mauri, M., Spagnolatti, M. and Garegnani, G., 2013. Management of flood hazard via hydro-morphological river modelling. The case of the M allero in Italian Alps. *Journal of Flood Risk Management* **6**(3): 197–209.

Ruiz-Villanueva, V., Badoux, A., Rickenmann, D., Bockli, M., Schläfli, S., Steeb, N., Stoffel, M. Rickli, C. 2018. Impacts of a large flood along a mountain river basin: the importance of channel widening and estimating the large wood budget in the upper Emme River (Switzerland). *Earth Surface Dynamics* **6**(4): 1115–1137.

Schumm, S.A., 1979. Geomorphic thresholds: the concept and its applications.

Transactions of the Institute of British Geographers New Series **4**: 485–515.

Milan, D., Schwendel, A. 2019. Long-term channel response to a major flood in an upland gravel-bed river. In *E-proceedings of the 38th IAHR World Congress*, 2831-2838). IAHR.

Schwendel, A., Milan, D.J. 2020. Terrestrial structure-from-motion: spatial error analysis of roughness and morphology. *Geomorphology* **350**: 106883.

Schwendel, A.C., Fuller, I.C., Death, R.G. 2012. Assessing DEM interpolation methods for effective representation of upland stream morphology for rapid appraisal of bed stability. *River Research and Applications* **28**(5): 567-584.

Scorpio, V., Crema, S., Marra, F., Righini, M., Ciccarese, G., Borga, M., Cavalli, M., Corsini, A., Marchi, L., Surian, N. Comiti, F. 2018. Basin-scale analysis of the geomorphic effectiveness of flash floods: a study in the northern Apennines (Italy). *Science of the Total Environment* **640**: 337-351.

Sear, D.A., Newson, M.D. 2003. Environmental change in river channels: a neglected element. Towards geomorphological typologies, standards and monitoring. *Science of the Total Environment* **310**: 17-23.

Skinner, C., Milan, D.J. 2018. Flash Flooding visualising the impacts. *Geography Review*, **31**.

Skinner, C.J., Coulthard, T.J., Schwanghart, W., Wiel, M.J., Hancock, G., 2018. Global sensitivity analysis of parameter uncertainty in landscape evolution models. *Geoscientific Model Development* **11**:4873-4888.

Slater, L.J. 2016. To what extent have changes in channel capacity contributed to flood hazard trends in England and Wales? *Earth Surface Processes and Landforms* **41**: 1115–1128.

- Surian, N., Righini, M., Lucía, A., Nardi, L., Amponsah, W., Benvenuti, M., Borga, M., Cavalli, M., Comiti, F., Marchi, L. Rinaldi, M. 2016. Channel response to extreme floods: insights on controlling factors from six mountain rivers in northern Apennines, Italy. *Geomorphology*, **272**: 78-91.
- The International Disaster Database. 2021. Centre for Research on the Epidemiology of Disasters (CRED). www.emdat.be
- Thompson, C., Croke, J. 2013. Geomorphic effects, flood power, and channel competence of a catastrophic flood in confined and unconfined reaches of the upper Lockyer valley, southeast Queensland, Australia. *Geomorphology*: **197**, 156-169.
- Van De Wiel, M.J., Coulthard, T.J., Macklin, M.G., Lewin, J. 2007. Embedding reach-scale fluvial dynamics within the CAESAR cellular automaton landscape evolution model. *Geomorphology* **90**(3-4): 283-301.
- Vischer, D., Hager, W.H. 1998. *Dam hydraulics* (Vol. 2). Chichester, UK: Wiley.
- Warburton, J., Kincey, M., Johnson, R.M. 2016. Assessment of Torrent Erosion Impacts on the Eastern Flank of Thirlmere Reservoir and A591 (Cumbria) Following Storm Desmond 2015. Durham University, Durham
- Wilby, R.L., Beven, K.J. Reynard, N.S. 2008. Climate change and fluvial flood risk in the UK: More of the same? *Hydrological Processes* **22**: 2511-2523.
- Wolman, M.G., Miller, J.P. 1960. Magnitude and frequency of forces in geomorphic processes. *Journal of Geology* **68**: 54-74.
- Wolman, M.G., Gerson, R., 1978. Relative scales of time and effectiveness of climate in watershed geomorphology. *Earth surface processes* **3**(2): 189-208.
- Wong, J. S., Freer, J. E., Bates, P. D., Sear, D. A., Step, E. 2015. Sensitivity of a hydraulic model to channel erosion uncertainty during extreme flooding. *Hydrological Processes* **29**: 261-279.

Accepted Article

Yu, D., Coulthard, T.J. 2015. Evaluating the importance of catchment hydrological parameters for urban surface water flood modelling using a simple hydro-inundation model. *Journal of Hydrology* **524**: 385-400.

Table 1 Point density for field surveys. Years 2003-2011 were undertaken using RTK-GPS survey, and 2014-2018 undertaken using terrestrial LiDAR.

Year	Survey density (points/m ²)
2003	0.91
2004	1.19
2007	1.76
2008	1.43
2011	2.32
2014	137
2015	516
2016	352
2017	380
2018	304

Table 2 Grain size and roughness information available for study reach.

*Measurements were derived from Wolman (1954) grid sampling of 5 representative morphological units in the study reach. [†]Measurements derived from the populations of grain roughness heights derived from terrestrial LiDAR point cloud data using 2σ of local elevations (Heritage and Milan, 2009).

Manning's n was calculated from D_{50} values using Equation 1.

Year	D_{50} (m)	Manning's n
2007*	0.080	0.031
2014 [†]	0.092	0.032
2015 [†]	0.090	0.032
2016 [†]	0.096	0.032
2017 [†]	0.084	0.031
2018 [†]	0.098	0.032

Table 3 Erosion and deposition volumes derived from DoD grids. *2003 to 2004 comparison is based only on the lower 250 m of the study reach due to the shorter surveyed length in 2003.

Period	Erosion (m ³)	Deposition (m ³)	Net volume change (m ³)
2003* to 2004	279	339	+60
2004 to 2007	2125	5202	+3077
2007 to 2008	2740	902	-1838
2008 to 2011	2033	2656	+623
2011 to 2014	1097	2641	+1544
2014 to 2015	112	128	+16
2015 to 2016	1121	725	-396
2016 to 2017	662	449	-213
2017 to 2018	357	521	+164

Graphical Abstract

Climate-change driven increased flood magnitudes and frequency in the British uplands: geomorphologically informed scientific underpinning for upland flood-risk management

David J. Milan¹ & Arved C. Schwendel²

